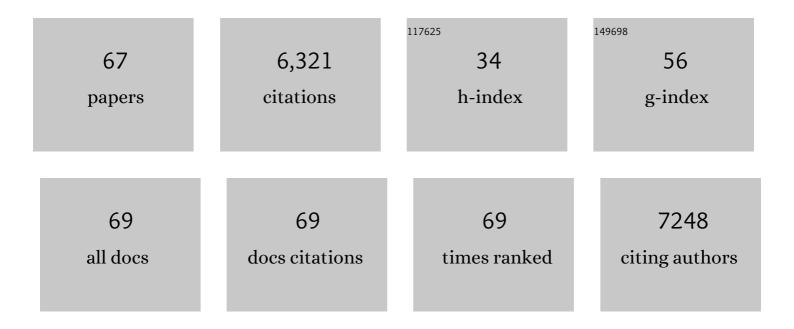
Chuanxiao Xiao

List of Publications by Year in descending order

Source: https://exaly.com/author-pdf/4376224/publications.pdf Version: 2024-02-01



#	Article	IF	CITATIONS
1	Efficient tandem solar cells with solution-processed perovskite on textured crystalline silicon. Science, 2020, 367, 1135-1140.	12.6	525
2	Employing Lead Thiocyanate Additive to Reduce the Hysteresis and Boost the Fill Factor of Planar Perovskite Solar Cells. Advanced Materials, 2016, 28, 5214-5221.	21.0	487
3	Extrinsic ion migration in perovskite solar cells. Energy and Environmental Science, 2017, 10, 1234-1242.	30.8	458
4	Efficient, stable silicon tandem cells enabled by anion-engineered wide-bandgap perovskites. Science, 2020, 368, 155-160.	12.6	420
5	Chiral-induced spin selectivity enables a room-temperature spin light-emitting diode. Science, 2021, 371, 1129-1133.	12.6	340
6	High efficiency perovskite quantum dot solar cells with charge separating heterostructure. Nature Communications, 2019, 10, 2842.	12.8	308
7	Spin-dependent charge transport through 2D chiral hybrid lead-iodide perovskites. Science Advances, 2019, 5, eaay0571.	10.3	275
8	Suppressing defects through the synergistic effect of a Lewis base and a Lewis acid for highly efficient and stable perovskite solar cells. Energy and Environmental Science, 2018, 11, 3480-3490.	30.8	274
9	Enhanced Charge Transport in 2D Perovskites via Fluorination of Organic Cation. Journal of the American Chemical Society, 2019, 141, 5972-5979.	13.7	274
10	Reducing Saturation urrent Density to Realize Highâ€Efficiency Lowâ€Bandgap Mixed Tin–Lead Halide Perovskite Solar Cells. Advanced Energy Materials, 2019, 9, 1803135.	19.5	255
11	Metastable Dion-Jacobson 2D structure enables efficient and stable perovskite solar cells. Science, 2022, 375, 71-76.	12.6	216
12	Cooperative tin oxide fullerene electron selective layers for high-performance planar perovskite solar cells. Journal of Materials Chemistry A, 2016, 4, 14276-14283.	10.3	204
13	Highly Distorted Chiral Two-Dimensional Tin Iodide Perovskites for Spin Polarized Charge Transport. Journal of the American Chemical Society, 2020, 142, 13030-13040.	13.7	198
14	Understanding and Eliminating Hysteresis for Highly Efficient Planar Perovskite Solar Cells. Advanced Energy Materials, 2017, 7, 1700414.	19.5	190
15	Low-bandgap mixed tin–lead iodide perovskites with reduced methylammonium for simultaneous enhancement of solar cell efficiency and stability. Nature Energy, 2020, 5, 768-776.	39.5	165
16	Mechanisms of Electron-Beam-Induced Damage in Perovskite Thin Films Revealed by Cathodoluminescence Spectroscopy. Journal of Physical Chemistry C, 2015, 119, 26904-26911.	3.1	153
17	Achieving a high open-circuit voltage in inverted wide-bandgap perovskite solar cells with a graded perovskite homojunction. Nano Energy, 2019, 61, 141-147.	16.0	152
18	A graded catalytic–protective layer for an efficient and stable water-splitting photocathode. Nature Energy, 2017, 2, .	39.5	135

CHUANXIAO XIAO

#	Article	IF	CITATIONS
19	Arylammonium-Assisted Reduction of the Open-Circuit Voltage Deficit in Wide-Bandgap Perovskite Solar Cells: The Role of Suppressed Ion Migration. ACS Energy Letters, 2020, 5, 2560-2568.	17.4	131
20	Self-Seeding Growth for Perovskite Solar Cells with Enhanced Stability. Joule, 2019, 3, 1452-1463.	24.0	120
21	Improving Charge Transport via Intermediateâ€Controlled Crystal Growth in 2D Perovskite Solar Cells. Advanced Functional Materials, 2019, 29, 1901652.	14.9	103
22	Efficient and Stable Graded CsPbI3â^'xBrx Perovskite Solar Cells and Submodules by Orthogonal Processable Spray Coating. Joule, 2021, 5, 481-494.	24.0	81
23	Enhancing Charge Transport of 2D Perovskite Passivation Agent for Wideâ€Bandgap Perovskite Solar Cells Beyond 21%. Solar Rrl, 2020, 4, 2000082.	5.8	79
24	Enhanced Charge Transport by Incorporating Formamidinium and Cesium Cations into Twoâ€Dimensional Perovskite Solar Cells. Angewandte Chemie - International Edition, 2019, 58, 11737-11741.	13.8	67
25	Basal Plane Hydrogen Evolution Activity from Mixed Metal Nitride MXenes Measured by Scanning Electrochemical Microscopy. Advanced Functional Materials, 2020, 30, 2001136.	14.9	63
26	Junction Quality of SnO ₂ -Based Perovskite Solar Cells Investigated by Nanometer-Scale Electrical Potential Profiling. ACS Applied Materials & Interfaces, 2017, 9, 38373-38380.	8.0	56
27	Unbiased solar H ₂ production with current density up to 23 mA cm ^{â[^]2} by Swiss-cheese black Si coupled with wastewater bioanode. Energy and Environmental Science, 2019, 12, 1088-1099.	30.8	48
28	Carbazole-Based Hole-Transport Materials for High-Efficiency and Stable Perovskite Solar Cells. ACS Applied Energy Materials, 2020, 3, 4492-4498.	5.1	47
29	Nanoscale mapping of hydrogen evolution on metallic and semiconducting MoS ₂ nanosheets. Nanoscale Horizons, 2019, 4, 619-624.	8.0	46
30	Nonpassivated Silicon Anode Surface. ACS Applied Materials & amp; Interfaces, 2020, 12, 26593-26600.	8.0	45
31	Templated Growth and Passivation of Vertically Oriented Antimony Selenide Thin Films for Highâ€Efficiency Solar Cells in Substrate Configuration. Advanced Functional Materials, 2022, 32, 2110032.	14.9	40
32	Inhomogeneous Doping of Perovskite Materials by Dopants from Hole-Transport Layer. Matter, 2020, 2, 261-272.	10.0	38
33	Individual Electron and Hole Mobilities in Lead-Halide Perovskites Revealed by Noncontact Methods. ACS Energy Letters, 2020, 5, 47-55.	17.4	37
34	Surface lattice engineering through three-dimensional lead iodide perovskitoid for high-performance perovskite solar cells. CheM, 2021, 7, 774-785.	11.7	37
35	Perovskite quantum dot solar cells: Mapping interfacial energetics for improving charge separation. Nano Energy, 2020, 78, 105319.	16.0	31
36	Emission Control from Transition Metal Dichalcogenide Monolayers by Aggregation-Induced Molecular Rotors. ACS Nano, 2020, 14, 7444-7453.	14.6	23

CHUANXIAO XIAO

#	Article	IF	CITATIONS
37	Enhanced Charge Transport by Incorporating Formamidinium and Cesium Cations into Twoâ€Dimensional Perovskite Solar Cells. Angewandte Chemie, 2019, 131, 11863-11867.	2.0	22
38	Lead-Free Flexible Perovskite Solar Cells with Interfacial Native Oxide Have >10% Efficiency and Simultaneously Enhanced Stability and Reliability. ACS Energy Letters, 2022, 7, 2256-2264.	17.4	19
39	Failure analysis of fieldâ€failed bypass diodes. Progress in Photovoltaics: Research and Applications, 2020, 28, 909-918.	8.1	18
40	Imaging, microscopic analysis, and modeling of a CdTe module degraded by heat and light. Solar Energy Materials and Solar Cells, 2018, 178, 46-51.	6.2	14
41	Electrochemically induced fractures in crystalline silicon anodes. Journal of Power Sources, 2019, 425, 44-49.	7.8	14
42	SMART Perovskite Growth: Enabling a Larger Range of Process Conditions. ACS Energy Letters, 2021, 6, 650-658.	17.4	14
43	Locating the electrical junctions in Cu(In,Ga)Se ₂ and Cu ₂ ZnSnSe ₄ solar cells by scanning capacitance spectroscopy. Progress in Photovoltaics: Research and Applications, 2017, 25, 33-40.	8.1	10
44	Super Flexible Transparent Conducting Oxideâ€Free Organic–Inorganic Hybrid Perovskite Solar Cells with 19.01% Efficiency (Active Area = 1 cm ²). Solar Rrl, 2021, 5, 2100733.	5.8	10
45	Near-field transport imaging applied to photovoltaic materials. Solar Energy, 2017, 153, 134-141.	6.1	9
46	Effect of Window-Layer Materials on p-n Junction Location in Cu(In,Ga)Se ₂ Solar Cells. IEEE Journal of Photovoltaics, 2019, 9, 308-312.	2.5	9
47	Module degradation mechanisms studied by a multi-scale approach. , 2016, , .		7
48	Development of in-situ high-voltage and high-temperature stressing capability on atomic force microscopy platform. Solar Energy, 2017, 158, 746-752.	6.1	7
49	Largeâ€Area Material and Junction Damage in c–Si Solar Cells by Potentialâ€Induced Degradation. Solar Rrl, 2019, 3, 1800303.	5.8	7
50	Carrier-Transport Study of Gallium Arsenide Hillock Defects. Microscopy and Microanalysis, 2019, 25, 1160-1166.	0.4	4
51	Light- and Elevated-Temperature-Induced Degradation-Affected Silicon Cells From a Utility-Scale Photovoltaic System Characterized by Deep-Level Transient Spectroscopy. IEEE Journal of Photovoltaics, 2022, 12, 703-710.	2.5	4
52	Area-Scalable Zn ₂ SnO ₄ Electron Transport Layer for Highly Efficient and Stable Perovskite Solar Modules. ACS Applied Materials & Interfaces, 2022, 14, 23297-23306.	8.0	4
53	Nanometer-scale electrical potential profiling across perovskite solar cells. , 2016, , .		3
54	In-situ Microscopy Characterization of Cu(In,Ga)Se ₂ Potential-Induced Degradation. , 2019, , .		3

#	Article	IF	CITATIONS
55	Nitride MXenes: Basal Plane Hydrogen Evolution Activity from Mixed Metal Nitride MXenes Measured by Scanning Electrochemical Microscopy (Adv. Funct. Mater. 47/2020). Advanced Functional Materials, 2020, 30, 2070313.	14.9	3
56	Direct Microscopy Imaging of Nonuniform Carrier Transport in Polycrystalline Cadmium Telluride. Cell Reports Physical Science, 2020, 1, 100230.	5.6	3
57	In-Operando Characterization of P-I-N Perovskite Solar Cells Under Reverse Bias. , 2021, , .		3
58	Development of scanning capacitance spectroscopy of CIGS solar cells. , 2015, , .		2
59	Enhancing Charge Transport of 2D Perovskite Passivation Agent for Wideâ€Bandgap Perovskite Solar Cells Beyond 21%. Solar Rrl, 2020, 4, 2070065.	5.8	2
60	LeTID-affected Cells from a Utility-scale Photovoltaic System Characterized by Deep Level Transient Spectroscopy. , 2021, , .		2
61	Linking Transient Voltage to Spatially-Resolved Luminescence Imaging to Understand Reliability of Perovskite Photovoltaics. , 2021, , .		2
62	Local Resistance Measurement for Degradation of c-Si Heterojunction with Intrinsic Thin Layer (HIT) Solar Modules. , 2020, , .		2
63	Metastable Dion-Jacobson 2D structure enables efficient and stable perovskite solar cells. Science, 2021, , eabj2637.	12.6	2
64	Longâ€Term Degradation of Passivated Emitter and Rear Contact Silicon Solar Cell under Light and Heat. Solar Rrl, 2022, 6, 2100727.	5.8	1
65	Determination of the electrical junction in Cu(In, Ga)Se <inf>2</inf> and Cu <inf>2</inf> ZnSnSe <inf>4</inf> solar cells with 20-nm spatial resolution. , 2016, , .		0
66	Large-Area Material and Junction Damage in c-Si Solar Cells by Potential-Induced Degradation. , 2018, , .		0
67	Carrier-Transport Imaging of Cadmium Telluride Intra- and Inter-Grains. , 2018, , .		0